



Mogrol Regulates the Expression of ATPase Na⁺/K⁺ Transport Subunit 3, Inhibits Cardiomyocyte Apoptosis, and Plays a Protective Role Against Myocardial Infarction

Feng Wang, Jinling Zhou, Weiwei Liu, Wei Wang, Boyan Tian, Jinyu Liu, Han Zhang, Peina He, Xiaoyun Yang , Li Yang, Yueheng Wang 

Echocardiology, The Second Hospital of Hebei Medical University, Shijiazhuang, Hebei, 050000, People's Republic of China

Correspondence: Yueheng Wang, Email 26500167@hebmu.edu.cn

Background: With the advancements in medical technology, the death rate from myocardial infarction (MI), a prevalent heart illness, has gradually decreased; however, treatment hurdles and diagnostic issues remain. Mogrol is a naturally occurring plant extract with specific biological activities such as antioxidant, anti-inflammatory, antitumor, and hypoglycemic effects. These biological activities make it a potential therapeutic drug or research subject; however, its function in MI remains unclear.

Methods: Potential targets of mogrol were searched using the MI Disease Database through online databases. Among the three intersecting genes, we focused on ATPase Na⁺/K⁺ transporting subunit 3A3, which is expressed at low levels in patients with MI. The preventive effect of mogrol against MI was investigated using cardiac ultrasonography, Western blotting, qPCR assay, Cell counting kit-8, Ca²⁺ concentration measurement, Na⁺/K⁺-ATPase, and flow cytometry.

Results: The findings demonstrated that mogrol upregulated Ca²⁺ concentration and ATPase Na⁺/K⁺ transporting subunit 3 protein levels in cardiomyocytes and tissues, downregulated the apoptosis-related proteins B-cell lymphoma 2-like protein 4, cleaved-caspase -3, and upregulated B-cell lymphoma 2. These effects enhanced cardiac function, prevented cardiomyocyte apoptosis, encouraged cardiomyocyte proliferation, and protected mice from MI. Knocking down ATP1A3 can reverse the protective effect of Mogrol.

Conclusion: Mogrol may have a protective effect on myocardial infarction by regulating Ca²⁺ concentration and the level of the ATPase Na⁺/K⁺ transport subunit 3 protein, as well as by regulating apoptosis-related proteins. Further revealing the pharmacokinetics of mogrol in vivo is expected to make it a subsequent drug for the treatment of cardiac infarction.

Keywords: mogrol, myocardial infarction, ATP1A3, apoptosis

Introduction

Myocardial infarction (MI) is a severe clinical condition with high mortality and morbidity rates. The morbidity and mortality of MI have increased in recent years due to changes in lifestyle and aging, which poses a serious threat to physical and mental health.^{1,2} Currently, medication, interventions, and surgery are the primary methods used to treat MI. Medication therapy includes antiplatelet medications, statins, angiotensin I converting enzyme inhibitors, β -blockers, and other medications that improve patient prognosis after MI. However, individual differences influence the effectiveness of pharmacological therapies, and prolonged drug use may result in negative effects.^{3,4} To effectively reduce the morbidity and mortality associated with MI, we need to further study the pathogenesis of MI and develop new treatment and prevention strategies.

MI is a serious cardiovascular disease caused by interruption of the coronary artery blood supply, resulting in myocardial ischemia and necrosis.⁵ Apoptosis, a type of programmed cell death, plays an important role in the development and occurrence of MI.⁶ According to the literature, myocardial cells are damaged by ischemia and hypoxia

after MI, thereby initiating apoptosis. Apoptosis can lead to a decrease in the number of myocardial cells, impaired myocardial function, ventricular remodeling, and even heart failure.^{7,8} Therefore, the inhibition of apoptosis is an important strategy for the treatment of MI.

The development of low-toxicity, high-efficiency medications can be aided by natural medicines, and *Siraitia grosvenorii* is a unique product found in Guangxi, China. Currently, Luo Han Guo is used to prepare Chinese herbal medications, beverages, and condiments that are highly valued both domestically and internationally.^{9,10} Mogrol is one of the single components extracted from Luo Han Guo, which has various pharmacological effects, including anti-inflammatory,¹¹ antitumor,¹² anti-osteoporosis,¹³ and neuroprotection.¹⁴ Mogrol is also a glycoside of Luo Han Guo Saponin, and it has been shown that Mogroside IIe can improve cardiomyocyte apoptosis and cardiac function in a rat model of type 2 diabetes mellitus.¹⁵ Therapeutic drugs for myocardial infarction have poor specificity and significant side effects with long-term use.^{3,4} Mogrol, with its natural advantages of low toxicity and high efficacy, has great potential for development.^{9,10} However, the effects of mogrol on cardiomyocytes and MI remain unknown. Based on bioinformatics analysis, we predicted the gene intersection of mogrol potential target genes and MI disease targets using an online database and focused on the intersection gene ATPase Na⁺/K⁺ transporting subunit 3 (*ATPIA3*). Molecular docking confirmed the existence of a binding site for mogrol and *ATPIA3*. *ATPIA3* encodes the $\alpha 3$ isoform of ATPase, an ion channel that is widely expressed in cardiomyocytes and has important effects on cardiac contraction and diastolic function. *ATPIA3* mutations have been reported in many neurological disorders of the brain, and the lack of *ATPIA3* expression is closely related to the onset and severity of brain diseases.^{16,17} Additionally, *ATPIA3* is associated with the susceptibility to bradycardia and ventricular fibrillation.¹⁸ A multicenter cohort study demonstrated an increased prevalence of abnormal electrocardiogram dynamics in *ATPIA3*-associated syndromes, and the risk of life-threatening rhythm abnormalities was comparable to that in established cardiac channelopathies (approximately 3%).¹⁹ This suggests that the *ATPIA3* deletion is a risk factor for MI and a potential bioindicator. However, *ATPIA3* in MI has not been reported. Therefore, we focused on the protective effect of mogrol against MI and the regulatory mechanism of *ATPIA3* with the aim of providing new therapeutic options and target genes for the treatment of MI.

Materials and Methods

GSE83500 Dataset Differential Gene Volcano and Heat Maps

The GSE83500 dataset was downloaded from the Gene Expression Omnibus database (<https://www.ncbi.nlm.nih.gov/gds>). Principal component analysis was performed on the two sets of samples using the R packages “FactoMineR” and “factoextra”.²⁰ Two sets of differential expressions were analyzed using the ‘limma’ package. A total of 1108 differentially expressed genes were obtained by screening according to a p-value < 0.05 and |logFC| > 1. The R package “ggplot2” was used to draw the differential gene volcano map, and the R package “pheatmap” was used to draw the Top20 differential gene volcano map.²¹

Venn Diagram and Protein-Protein Interaction Network Diagram

“LUO HAN GUO” was used as the keyword in the ETCM database (<http://www.tcmip.cn/ETCM/index.php/Home/>). We searched for *Siraitia grosvenorii*-related information, and then obtained the target of mogrol and downloaded the target information of mogrol and the differential gene (GSE83500) obtained in the previous section to draw the intersecting gene Wayne’s diagram using the Venn diagram package in R language.²² Using Cytoscape software, the proteins of the above intersecting gene interactions in the biogrid database were explored and visualized.

GO and KEGG Pathway Enrichment Analyses and Molecular Docking

The 2346 genes analyzed in the GSE83500 dataset were enriched for GO and KEGG functions using the R package “clusterProfiler”, and the top results are shown. The molecular structure of mogrol was obtained from the PubChem Compound Database (<https://pubchem.ncbi.nlm.nih.gov/>).²³ The 3D coordinates of ATP1A3 (PDB No. 8D3U) were downloaded from PDB (<http://www.rcsb.org/>), and molecular docking was performed using AutoDock Vina 1.2.2, a computerized protein-ligand docking software.

Cell Culture

Human cardiomyocytes AC16 were purchased from the Shanghai Cell Bank of the Chinese Academy of Sciences. Cells were removed from liquid nitrogen, resuscitated, and cultured in DMEM/F12 (a mixture containing 10% fetal bovine serum and 1% penicillin-streptomycin) medium. Mogrol (HY-N2312) was purchased from Med Chem Express Biotechnology, Inc.

In Vitro Modeling of MI

AC16 cells were cultured to the exponential phase, and mogrol (50 $\mu\text{mol/L}$) solution was added to pretreat the cells for 24 h. Cells were then placed in a 1% O_2 incubator and cultured for 12 h. The cells were incubated in a cell culture incubator for 12 h and extracted for subsequent experiments.

CCK-8 Assay

AC16 cells were cultured to the exponential phase, trypsin was added to digest the cells for 3 min, and the cell precipitate was collected. The cells were counted and inoculated in 96-well plates at a density of 3000/cells for culture and added with different concentrations of mogrol to incubate for 0, 24, 48, and 72 h, and then added with 10 μL of CCK-8 solution per well (Beyotime Biotechnology, C0038, China) and continued to incubate for 4 h. The 96-well plates were removed and placed on a SpectraMax Mini multifunctional enzyme labeling instrument to detect the optical density (OD; 450 nm).

EDU Staining Experiment

The cell sediment was collected as described previously, and the cells were counted as 5×10^6 cells per well inoculated in 6-well plates for overnight incubation, incubated for 24 h by adding mogrol (50 $\mu\text{mol/L}$) solution, incubated for 12 h with 1% O_2 , and added with an EDU staining solution for further 7 h. The cells were washed thrice with phosphate-buffered saline (PBS) for 5 min each. The cell fixative was added and incubated for 30 min, washed with PBS, incubated with Triton X-100 in a shaker for 10 min, incubated with DAPI for 5 min, washed with PBS, and photographed using an inverted fluorescence microscope (Sunny Optical Technology (Group) Co., Ltd, ICX41).

Cell Transfection

Take AC16 cells in the exponential growth phase, and inoculate the cells in a six-well plate at a density of 1×10^5 cells per well. According to the instructions of the transfection kit, mix Lip 3000 (Thermo Fisher Scientific, L3000075, China) with SiRNA and prepare it in a serum-free medium. Add the mixed solution to the AC16 cells and incubate for 3 h. Discard the old medium, replace it with fresh medium, and incubate overnight. After continuing to incubate for 48 h, the knockdown efficiency of ATP1A3 was verified by RT-qPCR and Western blot experiments. The sequence information of SiRNA is detailed in [Table S1](#).

qPCR Assay

After treatment, according to the requirements of different groups, the cell precipitate was extracted, the appropriate amount of Trizol solution was added, and total RNA was extracted according to the instructions. The NanoDrop One was used to determine the concentration of RNA, and reverse transcription was used to obtain cDNA according to the requirements of the BeyoRT™ II cDNA First Strand Synthesis Kit (Beyotime Biotechnology, D7168M, China). cDNA was added to the premixed solution of BeyoFast™ SYBR Green qPCR Mix (Beyotime Biotechnology, D7262, China), the ABI 7900HT fluorescence PCR instrument was set up according to the instruction manual, and then the results were analyzed with the software provided by the fluorescence PCR instrument after completion of the operation.²⁴ The primer sequences are detailed in [Table S1](#).

Flow Cytometry

The treated cell precipitate was extracted, the cells were resuspended with PBS, 5 μL of Annexin V-FITC was added and mixed, 10 μL of propidium iodide was added and mixed, and the solution was incubated for 20 min at room temperature in the dark. The cells were detected using flow cytometry (BD FACSCanto™), and after that, the apoptosis rate was statistically analyzed using Flow Jo.

Na⁺/K⁺-ATPase and Ca²⁺ Concentration Measurements

Treated cell samples and mouse myocardial tissues were extracted, and the tissues and cells were lysed using ultrasound. The Na⁺/K⁺-ATPase Assay Kit (Solarbio, BC0065) and Ca²⁺ Concentration Assay Kit (ab102505; Abcam) were used according to the manufacturers' requirements. Cell and tissue samples were processed separately, and Na⁺/K⁺-ATPase OD values were detected at 660 nm and Ca²⁺ OD values at 575 nm using an enzyme marker (Read Max 1200), and the data were recorded for subsequent statistical analysis.

Western Blot Assay

Cell precipitation was performed by adding tissue cell lysate to incubate the cells and tissue samples for 30 min, extracting the protein solution, determining the protein concentration using a BCA kit, adjusting the amount of sample according to the protein concentration, adding an equal amount of protein solution to the grooves of the gel, setting the voltage at 120 V to perform gel electrophoresis, after 75 min the gel was transferred to a polyvinylidene fluoride (PVDF) membrane, after which the conditioned voltage was adjusted to 200 V, and the PVDF membrane was incubated for 2 h with a primary antibody overnight and washed three times with TBST. After 30 min, the PVDF membranes were incubated with 5% skim milk powder for 2 h. At the end of the incubation, the membrane was washed three times with TBST, incubated overnight with the primary antibody, washed three times with TBST, and incubated with the secondary antibody for 2 h. After incubation with the secondary antibody for 2 h, a chemiluminescent solution was added and incubated for 10s. The images were then placed in a chemiluminescent instrument and preserved for subsequent statistical analyses. ATP1A3 (#DF9942), Bax (#AF0120), Bcl-2 (#AF6139), cleaved-caspase-3 (#AF7022), GAPDH (#AF7021), Goat Anti-Rabbit IgG (H+L) HRP (#S0001), and Goat Anti-Mouse IgG (H+L) HRP (#S0002) were purchased from Affinity Biosciences, USA.

In Vivo Experiment

A total of 48 male C57BL/6 mice aged 6–8 weeks and with a body weight of 20–28 g were kept in the animal experiment of the Fourth Hospital of Hebei Medical University. Adequate sterile feed and water were provided, and the formal experiment started after seven days of feeding. The experiment was randomly divided into four groups: Control (sham operation group), MI group (myocardial infarction model group), Mogrol group (treated with Mogrol alone), MI + Mogrol group (myocardial infarction model mice + treated with Mogrol). The Mogrol and Mogrol+MI groups were injected intraperitoneally with 20 mg/kg rotenoneol suspension one day before infarction surgery, and the other groups were injected with the same volume of saline. On the following day, the MI model was constructed using the left anterior descending ligation method, and the MI and Mogrol group+MI groups were anesthetized by inhaling 2% isoflurane. The chest was incised with a horizontal incision, the left anterior descending was ligated with a 7-0 nylon suture, and mice in the other groups underwent the same surgery without ligation.²⁵ The postoperative status of the mice was observed daily, after which mice in the Mogrol and Mogrol+MI groups were injected intraperitoneally with 20 mg/kg mogrol suspension every three days, and mice in the other groups were injected with the same volume of saline. Mice with a body weight loss of more than 10% compared to the previous day or with severe clinical symptoms were euthanized in accordance with the institutional animal ethics guidelines, and the date of death was recorded as the next day. After four weeks, some mice died as a result of the MI surgery; therefore, six mice from each group of surviving mice were randomly selected for subsequent experiments. An animal ultrasound system was used to detect the cardiac ultrasound of mice. To detect the functional indices of the mouse heart, the myocardial tissues of mice were subjected to hematoxylin and eosin staining.

Cardiac Ultrasound

For echocardiography, the animals were anesthetized under gas anesthesia (isoflurane-vi fluorane, Virbac 1.8–2% in a 1:1 oxygen:air mixture). Hair was removed from the thoracic area (depilatory cream was used for sensitive skin), and the animals were placed on a heated platform connected to an ultrasound system (Vevo[®] 3100 LT, 69 Fujifilm VisualSonics Inc., Toronto, Canada) to record electrocardiogram and respiratory rate.²⁶ Images were acquired using a 70 MS-550D (55 MHz) transducer, specifically designed for cardiac imaging in mice (VisualSonics), to determine the AT:ET ratio and CO.

Hemodynamic parameters were measured in non-ventilated anesthetized mice using a closed-chest technique by introducing a 1.4 f Miller catheter (AD Instruments, Paris, France) into the jugular vein and directing it to the right ventricle via inhalation of 2.0% isoflurane in room air.²⁷ After completing the hemodynamic assessment, the mice were sacrificed to dissect the myocardial tissue, and cardiac function indices were recorded for subsequent statistical analysis.

Statistical Analysis

Data analysis was performed using GraphPad Prism 9.5.0 software. Measured data were expressed as mean \pm standard deviation (SD). For the results of Western blot analysis and CCK-8 data, two-way analysis of variance (ANOVA) was first used for evaluation. Before conducting ANOVA, normality tests (using the Shapiro–Wilk test) and homogeneity of variance tests (using the Levene test) were performed on the data. If the data met the assumptions of normality and homogeneity of variance, ANOVA was directly conducted; if not, appropriate transformations of the data (such as logarithmic transformation) were performed to meet the assumptions. If still not met, non-parametric test methods (such as the Kruskal–Wallis test) were used. After ANOVA showed significant differences among groups, Tukey’s honest significant difference test was used for multiple comparisons to control the type I error rate. For other data, one-way analysis of variance was used for evaluation. Similarly, normality and homogeneity of variance tests were performed before the analysis, and the processing methods were the same as above. Then, post hoc comparisons were conducted with Tukey’s honest significant difference test. A P value less than 0.05 was considered statistically significant. The sample size of each experiment was carried out as an independent experiment for each repetition, and the sample size was no less than 5 independent observations.

Results

Screening of Potential Therapeutic Targets of Mogrol in MI

The GSE83500 dataset was downloaded from the Gene Expression Omnibus database (<https://www.ncbi.nlm.nih.gov/gds>). Principal component analysis was performed on the GSE83500 dataset. The results showed that the ellipses of the disease group and the healthy group did not overlap, indicating a significant difference between the two groups (Figure 1A). The volcano plot (Figure 1B), clustering heatmap (Figure 1C), Gene Ontology (GO) functional enrichment plot (Figure 1D), and Kyoto Encyclopedia of Genes and Genomes (KEGG) functional enrichment plot (Figure 1E) of this dataset were plotted; however, we did not find any information of interest. Subsequently, we downloaded the mogrol-predicted target information from the Encyclopedia of Traditional Chinese Medicine (ETCM) database to determine gene intersection with the GSE83500 database. Figure 1F plots the Venn diagram of the three intersecting genes, and only interleukin (IL)-6 and ATP1A3 had proteins that interacted with them, IL-6 had four proteins that interacted with it, and ATP1A3 had 37 interacting proteins (Figure 1G). The role of IL-6 in myocardial infarction has been widely studied, and its mechanism is relatively clear, leaving relatively limited space for further in-depth exploration.²⁸ However, the role of ATP1A3 in myocardial infarction has not been fully explored and has greater research potential. Currently, research on SLC1B3 is very limited, and there is not even a single report related to heart diseases. Although this may indicate that this gene has high research value, the lack of basic data and research background makes it difficult for us to determine its specific mechanism of action in myocardial infarction. In contrast, there is already a considerable research basis for ATP1A3, which will help us advance the research more quickly. Therefore, we focused on ATP1A3 to further validate the relationship between mogrol and ATP1A3. Our molecular docking results showed that mogrol binds to ATP1A3 with a binding energy of -8.7 kcal/mol, an excellent binding capacity. This further confirms that ATP1A3 may be the binding site for mogrol (Figure 1H).

Mogrol Restores the Proliferative Capacity of AC16 Cells

The qPCR results showed that ATP1A3 mRNA expression was significantly downregulated and statistically significant in the model group compared with that in the control group in AC16 cells, whereas there was no significant difference in IL-6 and solute carrier organic anion transporter family member SLC1B3 (Figure 2A). The 2D and 3D molecular structures of mogrol are shown in Figure 2B. The downregulation of ATP1A3 in the model group was in accordance with the results from the GSE83500 database (Table 1). We simulated an in vivo MI model by treating AC16 cells with

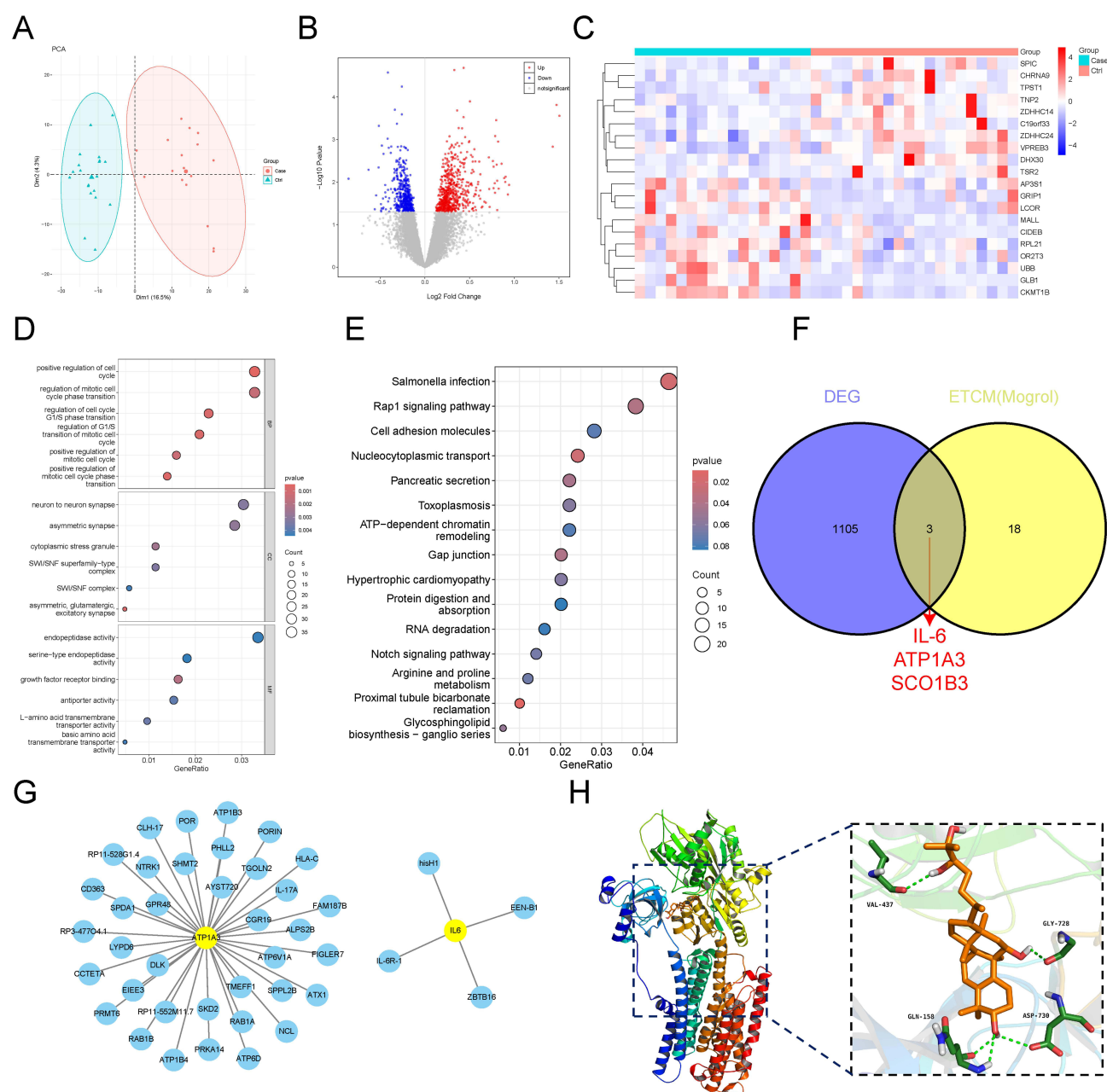


Figure 1 Analysis of mogrol-predicted targets and MI targets. **(A)** Principal component analysis (PCA) was performed using two sets of samples from the GSE8350 database. **(B)** Volcano diagram. **(C)** Clustered heat map. **(D)** GO functional enrichment analysis. **(E)** KEGG functional enrichment analysis. **(F)** Venn diagram showing the intersection of the identified genes between the GSE8350 and ETCM databases. **(G)** Proteins that explored the interactions of the above intersecting genes in the biogrid database were explored and visualized using the Cytoscape software. **(H)** The docking binding energy of ATP1A3 and mogrol is -8.7 kcal/mol.

hypoxia in vitro, and to determine the nontoxic concentration of mogrol, we treated AC16 cells with different concentrations of mogrol for 48 h. The cell counting kit-8 (CCK-8) results showed that there were no significant differences in cell viability between 6.25–50 $\mu\text{mol/L}$ compared with the control group, whereas between 100–200 $\mu\text{mol/L}$ mogrol had an inhibitory effect on AC16 cell proliferation (Figure 2C). Therefore, the mogrol concentration selected was 50 $\mu\text{mol/L}$ for subsequent experiments. We found that mogrol (50 $\mu\text{mol/L}$)-pretreated AC16 cells were able to alleviate the inhibition of cell proliferation brought about by hypoxia treatment (Figure 2D), and the results of EDU experiments further confirmed the protective effect of mogrol on AC16 cell proliferation (Figure 2E).

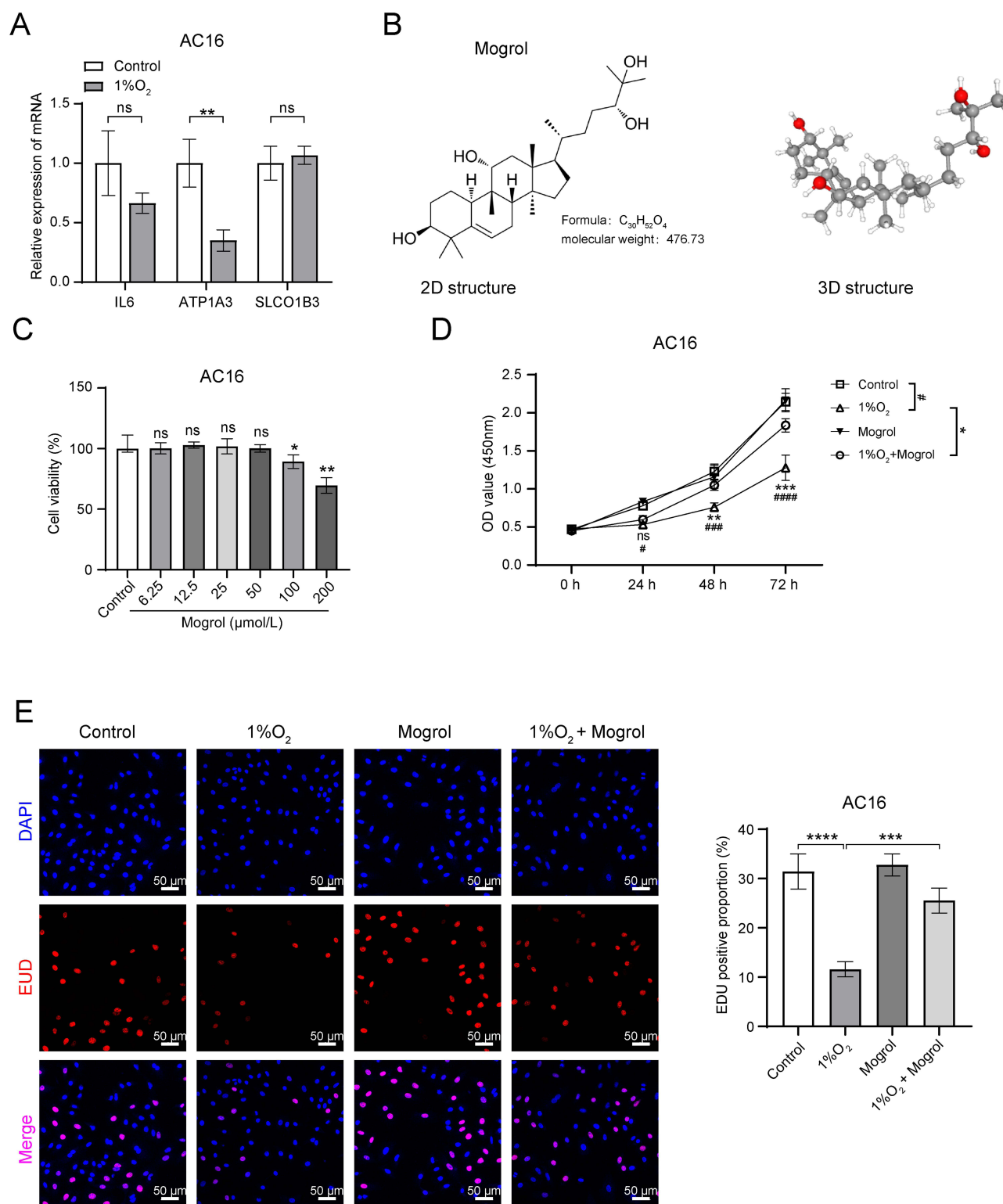


Figure 2 Mogrol enhances cell viability of AC16 cells in hypoxic conditions. (A) qPCR experiments were performed to detect the expression levels of *IL-6*, *ATP1A3*, and *SLCO1B3* mRNA in AC cells after 12 h of hypoxic treatment. (n=6) (B) Structural formula and relative molecular mass of 2D and 3D mogrol molecules. (C) CCK-8 detection of changes in cell viability of AC16 cells after treatment with different concentrations of mogrol for 48 h. (n=6) (D) CCK-8 detection of changes in cell viability of AC16 cells under hypoxia by mogrol pretreatment. (n=6) (E) EDU staining to observe the effect of mogrol pretreatment on the proliferation of AC16 cells under hypoxia (n=6). (* $P < 0.05$, ** $P < 0.01$, *** $P < 0.001$, **** $P < 0.0001$).

Table 1 Intersection Gene Expression Profiles

	logFC	P.Value	Change
IL6	−0.242233717	0.00329098	Down
ATPIA3	−0.189902377	0.03342232	Down
SLCO1B3	0.27550498	0.014204761	Up

Mogrol Improves Cardiac Function and Survival in MI Mice

After the initial confirmation of the protective effect of mogrol *in vitro*, an MI mouse model was constructed *in vivo* to further confirm our hypothesis. The flowchart of myocardial infarction modeling and mogrol treatment is shown in [Figure 3A](#). We evaluated the cardiac function of the mice using echocardiography and found no significant change in heart rate, a significant decrease in ejection fraction and fractional shortening, narrowing of left ventricular end-diastolic anterior wall thickness and left ventricular end-diastolic posterior wall thickness, and thickening of left ventricular end-systolic diameter and left ventricular end-diastolic diameter in the MI group compared with the control group ([Figure 3B and D](#)). The cardiac function of MI mice was significantly improved by mogrol treatment, and the survival rate of mice in each group was observed. Within 30 days, mortality increased in the MI group, whereas mogrol treatment reduced mortality after MI ([Figure 3C](#)). Our findings strongly suggest that mogrol has a therapeutic effect on the cardiac function and survival of MI mice.

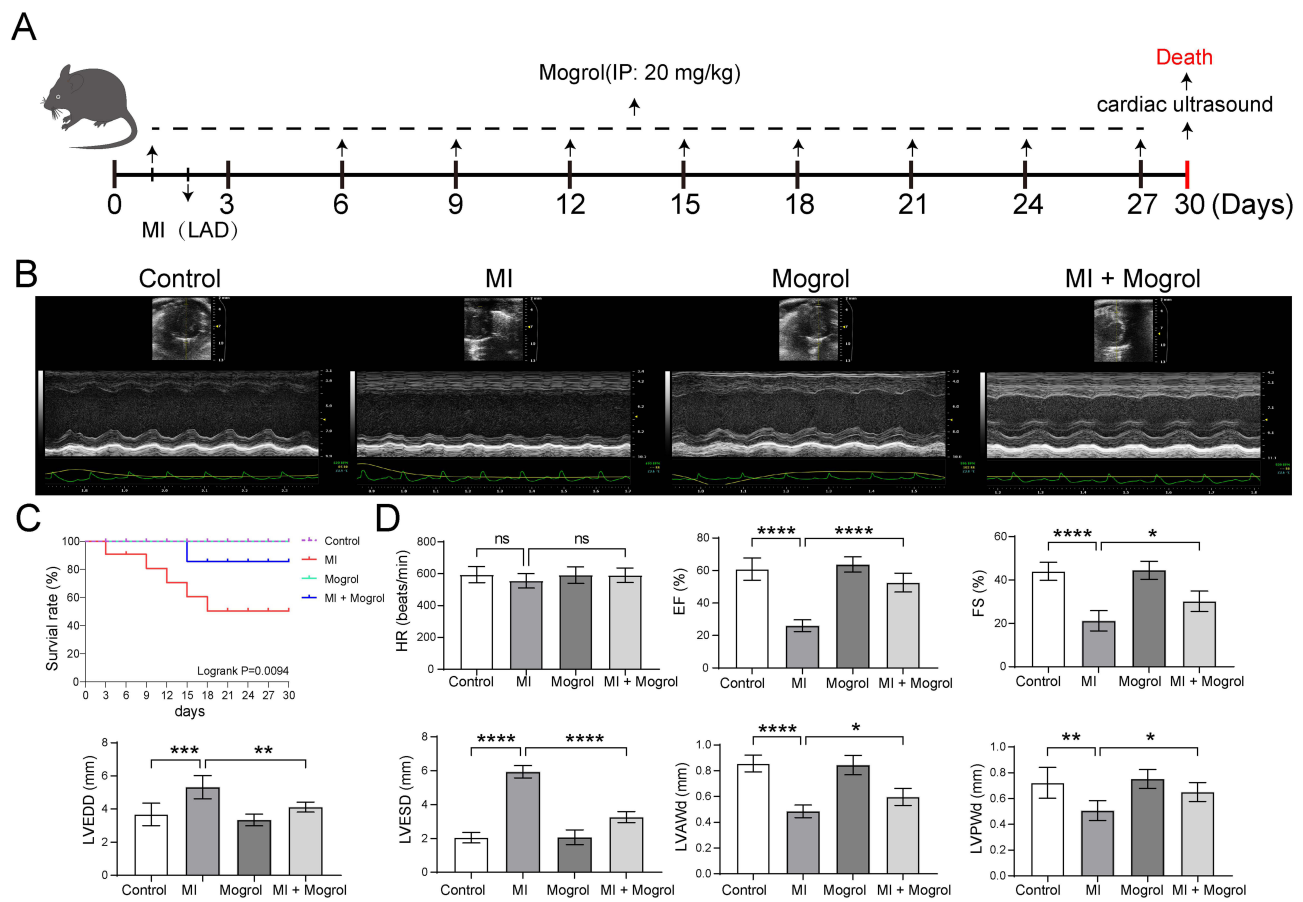


Figure 3 Mogrol improves cardiac function in MI mice. **(A)**Flowchart of the *in vivo* MI mouse experiments. **(B)** Cardiac ultrasound of the MI mice. (n=6) **(C)** Prognostic survival curves of MI mice. (n=12)**(D)** Changes in the expression of cardiac function indices, including HR, EF (%), FS (%), LVEDD (mm), LVESD (mm), LVAWd (mm), and LVPWd (mm), in mice (n=6). (* $P < 0.05$, ** $P < 0.01$, *** $P < 0.001$, **** $P < 0.0001$) Interpretation of nouns. **Abbreviations:** Heart rate (HR); Left ventricular end-systolic diameter (LVESD); Left ventricular end-diastolic diameter (LVEDD); Ejection fraction (EF); Fractional shortening (FS); Left ventricular end-diastolic anterior wall thickness (LVAWd); Left ventricular end-diastolic posterior wall thickness (LVPWd).

Mogrol Inhibits Myocardial Tissue and AC16 Cell Apoptosis in MI Mice

The effect of mogrol pretreatment on apoptosis was verified in the AC16 MI model. The results of the flow cytometry assay for apoptosis showed that the apoptosis percentage was significantly higher in the 1%O₂ group than in the control group, whereas the apoptosis percentage was significantly lower in the 1%O₂+Mogrol group than in the 1%O₂ group (Figure 4A). These results demonstrated that pretreatment with mogrol prevented hypoxia-induced apoptosis in AC16 cells. We next explored the possible mechanism of action of mogrol and found that it was able to activate the expression of ATP1A3 protein in the 1%O₂+Mogrol group compared with the 1%O₂ group. In addition, it induced the upregulation of the

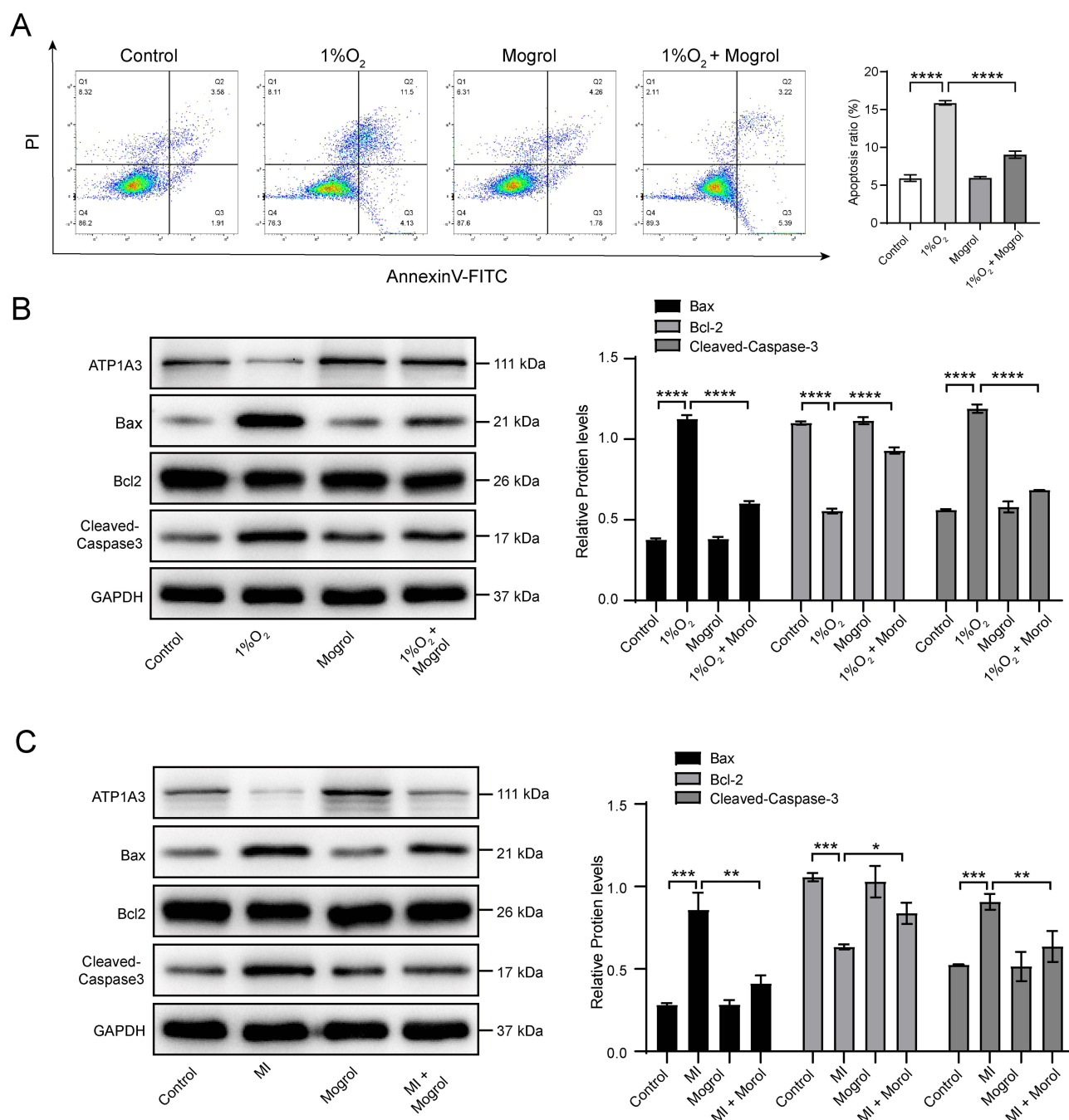


Figure 4 Mogrol inhibits cardiomyocyte apoptosis in vitro and in vivo. (A) Flow double staining to detect changes in cardiomyocyte apoptosis. (n=6) (B) Western blotting to detect changes in the expression of ATP1A3 and apoptosis-related proteins Bax, Bcl-2, and cleaved-caspase-3 in AC16 cells. (n=6) (C) Western blotting was performed to detect changes in the expression of ATP1A3 and apoptosis-related proteins Bax, Bcl-2, and cleaved-caspase-3 in myocardial tissues (n=6). (* $P < 0.05$, ** $P < 0.01$, *** $P < 0.001$, **** $P < 0.0001$).

expression levels of apoptotic proteins B-cell lymphoma 2 (Bcl-2)-like protein 4 (Bax) and cleaved-caspase-3 and inhibited the downregulation of the expression level of the apoptotic protein Bcl-2 (Figure 4B and C). These results further confirm that mogrol can resist apoptosis induced by hypoxia and that this process may act through the activation of the ATP1A3 protein. In AC16 cells, mogrol rescued the hypoxia-induced decrease in Na^+/K^+ -ATPase and Ca^{2+} concentrations.

Mogrol Activates ATP1A3, Which in Turn Upregulates Na^+/K^+ -ATPase and Ca^{2+} Concentrations

We examined the expression level of ATP1A3 protein using Western blotting and examined Na^+/K^+ -ATPase and Ca^{2+} concentrations. The results showed that mogrol upregulated the protein and mRNA expression levels of ATP1A3 and enhanced the Na^+/K^+ -ATPase and Ca^{2+} concentrations in myocardial tissues and AC cells (Figure 5A–D). The therapeutic effect of mogrol on myocardial tissues was most likely mediated by activating the expression of ATP1A3 and rescuing the MI model in vivo and ex vivo, resulting in a decrease in Na^+/K^+ -ATPase expression and Ca^{2+} concentration, exerting a protective effect on cardiomyocytes.

Mogrol Resists Apoptosis in Mouse Myocardial Tissues and AC Cells by Enhancing ATP1A3 Protein Expression

To further confirm that Mogrol resists cardiomyocyte apoptosis by activating ATP1A3 protein expression, we constructed an ATP1A3 knockdown cell line in AC16 cells. The results of Western blot and RT-qPCR showed that siATP1A3-1, siATP1A3-2, and siATP1A3-3 could downregulate the relative expression levels of ATP1A3 protein and mRNA in AC16 cells to varying degrees. Among them, siATP1A3-2 had the strongest knockdown effect on ATP1A3 protein and mRNA (Figure 6A). Therefore, we used siATP1A3-2 as the experimental group for ATP1A3 knockdown and siNC as the control group for Knockdown in the subsequent studies. The results of detecting cell apoptosis by flow cytometry showed that Mogrol could resist hypoxia-induced apoptosis of AC16 cells. And knockdown of ATP1A3 could reverse the resistance effect of Mogrol on AC16 cell apoptosis (Figure 6B). The results suggest that Mogrol resists AC16 cell apoptosis by

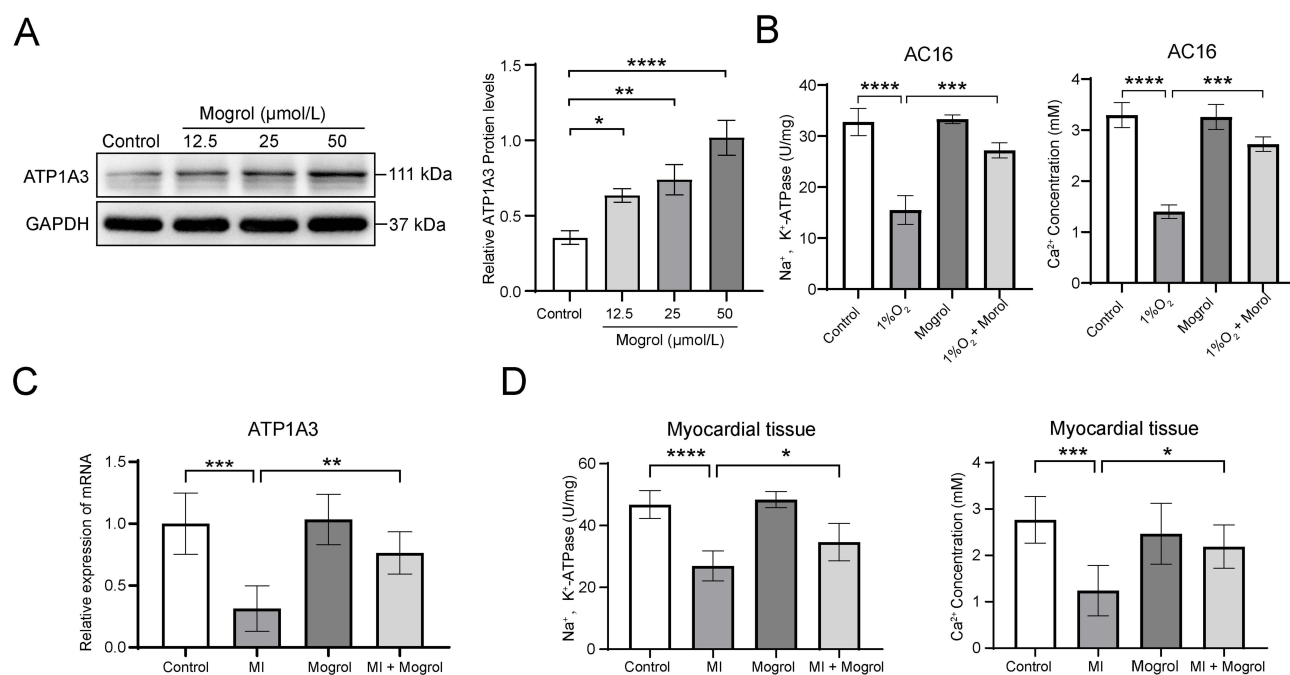


Figure 5 Mogrol enhances Na^+/K^+ -ATPase levels and Ca^{2+} concentration. (A) Western blot analysis of ATP1A3 protein expression in AC16 cells treated with different concentrations of mogrol. (n=6) (B) Detection of Na^+/K^+ -ATPase levels and Ca^{2+} concentrations in AC16 cells after mogrol treatment. (n=6) (C) Changes in ATP1A3 mRNA expression in cardiomyocytes after mogrol treatment. (n=6) (D) Detection of Na^+/K^+ -ATPase levels and Ca^{2+} concentration in cardiomyocytes after mogrol treatment (n=6). (* $P < 0.05$, ** $P < 0.01$, *** $P < 0.001$, **** $P < 0.0001$).

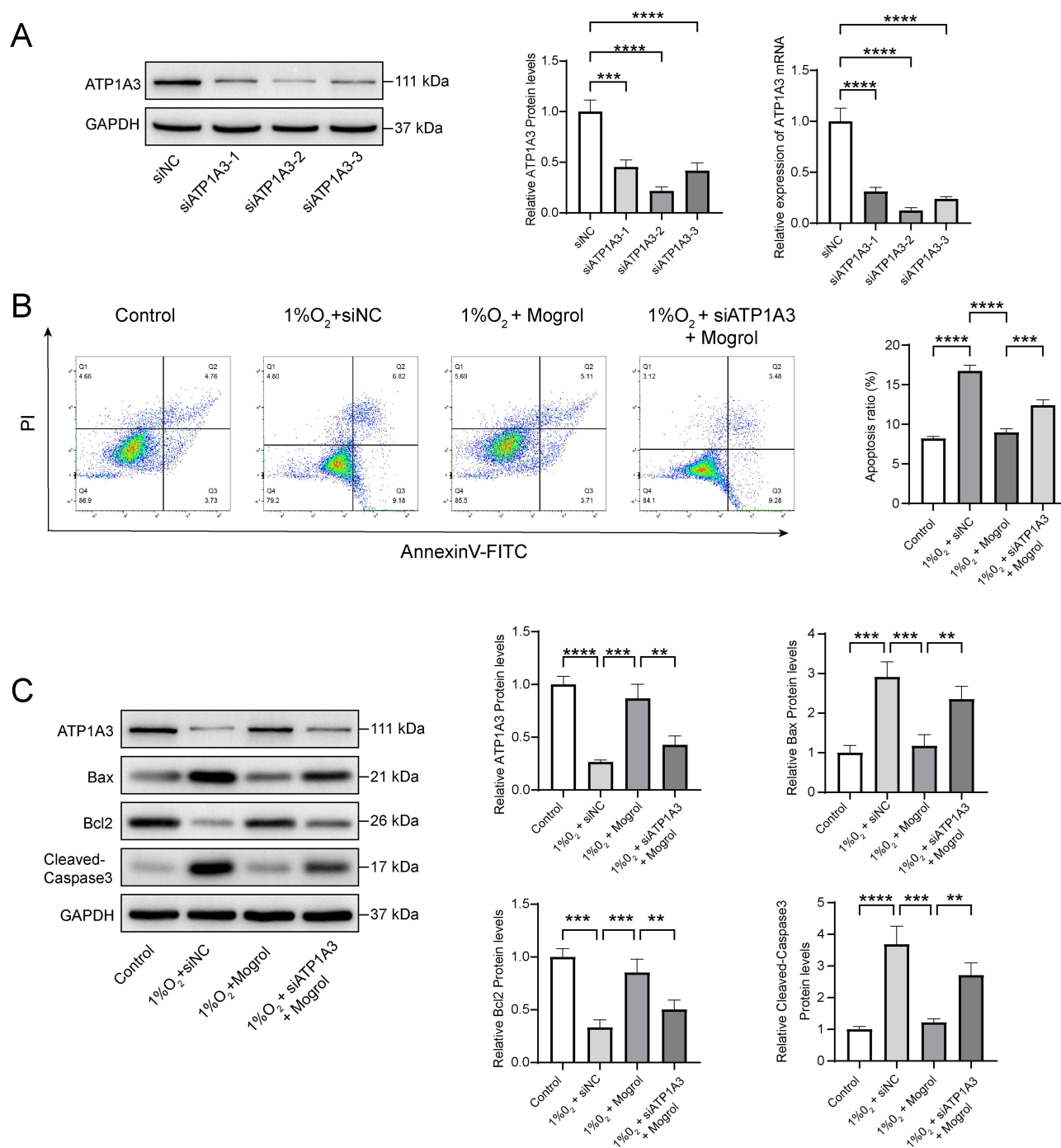


Figure 6 Mogrol targets and activates ATP1A3 to resist cardiomyocyte apoptosis. **(A)** Western blot was used to detect the relative expression level of ATP1A3 protein in AC16 cardiomyocytes 48 hours after transfection with siRNA. (n = 6) **(B)** Flow cytometry was used to detect the changes in apoptosis of AC16 cells transfected with siRNA after treatment with Mogrol under hypoxia induction. (n = 6) **(C)** Western blot was used to detect the relative expression changes of ATP1A3, Bax, Bcl-2, and Cleaved-caspase3 proteins in each experimental group. (n = 6) (* $P < 0.01$, ** $P < 0.001$, *** $P < 0.0001$).

targeting and activating ATP1A3. To further strengthen this conclusion, we detected the expression levels of apoptosis-related proteins by Western blot experiments. We found that Mogrol could downregulate Bax and Cleaved-caspase-3 and upregulate the relative expression levels of Bcl-2 and ATP1A3 proteins. And knockdown of ATP1A3 could reverse the regulatory effect of Mogrol on apoptosis-related proteins (Figure 6C). The results further strengthened the conclusion that Mogrol resists AC16 cell apoptosis by targeting and activating ATP1A3.

Discussion

Mogrol, with its natural advantages of low toxicity and high efficacy, has become a drug candidate for various diseases,²⁹ and its derivatives have shown great potential in the anticancer field.³⁰ Mogrol has not been previously reported in the field of MI, and the most innovative aspect of this study was to reveal the therapeutic and protective effects of mogrol in mice with MI. Based on the results of online database analysis, we identified *ATPIA3* as a potential target of mogrol, and molecular docking and qPCR experiments further confirmed the existence of a regulatory relationship between mogrol and *ATPIA3*. In addition, *ATPIA3* expression was downregulated in the MI Disease Database, which is consistent with the results reported by Yin et al, who showed that Na^+/K^+ -ATPase expression was significantly reduced in patients with acute MI ($P < 0.05$).³¹ Ventricular fibrillation and arrhythmia are also common in pediatric patients with alternating hemiparesis, and researchers have suggested that this may be related to the lack of *ATPIA3* expression.¹⁴ Our ex vivo and in vivo studies have shown that the MI model inhibits cardiomyocyte proliferation, induces apoptosis, and downregulates ATP13A expression. In contrast, mogrol rescued the ATP1A3 expression deficiency and improved cardiac function in the MI model. Recent studies have shown that Na^+/K^+ -ATPase not only actively transports sodium and potassium ions across the membrane but also has a signal transduction function to maintain the resting potential of cardiomyocytes.³² Calcium pumps activate various intracellular calcium pumps. Calcium pumps activate various intracellular signaling pathways to maintain diastolic and systolic homeostasis.³³ We found that the MI model blocked the activity of Na^+/K^+ -ATPase and Ca^{2+} and that mogrol treatment reversed this effect. Our findings preliminarily elucidated a possible mechanism of mogrol treatment in MI.

During MI, owing to the obstruction of coronary arteries, cardiomyocyte ischemia, hypoxia, and mitochondrial dysfunction, a large number of cardiomyocytes undergo apoptosis, which is also an important factor in inducing MI.³⁴ Reducing Bax/Bcl-2 expression has been shown to alleviate MI and apoptosis.^{35,36} As expected, mogrol reduced Bax/Bcl-2 expression and downregulated cleaved-caspase-3 expression in cardiomyocytes in the MI model. The decrease in Bax/Bcl-2 leads to the release of the mitochondrial matrix into the cellular stroma, which induces the upregulation of cleaved-caspase-3, directly leading to apoptotic cell death.³⁷ We hypothesize that mogrol is likely to inhibit the classical mitochondrial apoptotic pathway and thus inhibit cardiomyocyte apoptosis. Furthermore, mogrol may also act through other pathways, such as mitochondrial function, oxidative stress, or inflammatory signals, etc. Of course, this still requires a large number of functional and mechanistic experiments for further confirmation. Furthermore, we also focused on the safety and efficacy of mogrol. We found that the sole treatment of mogrol had no impact on the cardiac-related functional indicators and myocardial tissue apoptosis of mice, which preliminarily confirmed the safety of mogrol in in vivo administration. Compared with the drug doses of other natural compounds in myocardial infarction mice, such as Mangiferin (40 mg/kg),³⁸ Cyanidin (30 mg/kg),³⁹ and Colchicine (100 mg/kg),⁴⁰ Mogrol has a relatively good therapeutic effect on myocardial infarction at a drug dose of 20 mg/kg. Based on these findings, future therapeutic strategies targeting *ATPIA3* are of great value. Mogrol intervention regulates *ATPIA3* expression and improves myocardial function, making it a novel therapeutic option.

In conclusion, this is the first study to demonstrate that mogrol activates ATP1A3 expression and attenuates cardiomyocyte apoptosis in an MI model. Although our findings are encouraging, there are some limitations. In our study, the small sample size in each group limited the credibility of our conclusion. In the future, the sample size of in vivo studies should be expanded to further confirm our conclusion. The bioavailability of mogrol is low, water solubility is poor, and higher doses are required to achieve effective concentrations. The in vivo metabolic process of mogrol is unknown and may affect its efficacy and safety. In addition, the mechanism of action of mogrol in the treatment of MI remains unclear and needs to be further verified by designing a large number of experiments. Mogrol, a compound with potential for cardiovascular protection, faces a key challenge in clinical application due to its low bioavailability. To address this, approaches like enhancing the physicochemical properties of the drug, employing nanotechnology, carrying out structural modifications, and optimizing the dosing regimen could be contemplated to raise its bioavailability. Additionally, comprehending the in vivo metabolic process of Mogrol is of paramount importance for optimizing drug design and enhancing clinical efficacy. Future research is required to further explore the in vivo metabolic characteristics of Mogrol and its mechanism of action in myocardial infarction, thereby providing more scientific grounds for clinical application.

Conclusion

In conclusion, we have confirmed that Mogrol can resist the apoptosis of myocardial tissues and AC16 cells and play a protective role in myocardial infarction. The possible mechanism is through activating the ATP1A3 protein. Mogrol is expected to provide new strategies and methods for the prevention and treatment of myocardial infarction. However, the bioavailability and pharmacokinetic studies of Mogrol still need to be further conducted to provide more information for its clinical application.

Abbreviations

ATP1A3, ATPase Na⁺/K⁺ transporting subunit 3; Bax, B-cell lymphoma 2-like protein 4; Bcl-2, B-cell lymphoma 2; CCK-8, cell counting kit-8; ETCM, Encyclopedia of Traditional Chinese Medicine; GAPDH, glyceraldehyde-3-phosphate dehydrogenase; GO, Gene Ontology; IL, interleukin; KEGG, Kyoto Encyclopedia of Genes and Genomes; MI, myocardial infarction; OD, optical density, PVDF, polyvinylidene fluoride.

Ethics Approval and Consent to Participate

The authors are accountable for all aspects of the work in ensuring that questions related to the accuracy or integrity of any part of the work are appropriately investigated and resolved. All animal experiments were performed under a project license (2023-AE314) granted by animal ethics committee of Second Hospital of Hebei Medical University, in compliance with institutional guidelines for the care and use of animals. For the online database analysis involving humans in this study, it complies with the requirements for exemption from ethical approval according to Items 1 and 2 of Article 32 of the “Measures for Ethical Review of Life Science and Medical Research Involving Human Subjects” in China on February 18, 2023.

Author Contributions

All authors made a significant contribution to the work reported, whether that is in the conception, study design, execution, acquisition of data, analysis and interpretation, or in all these areas; took part in drafting, revising or critically reviewing the article; gave final approval of the version to be published; have agreed on the journal to which the article has been submitted; and agree to be accountable for all aspects of the work.

Disclosure

The authors have no conflicts of interest to declare.

References

- Christensen DM, Strange JE, El-Chouli M, et al. Temporal trends in noncardiovascular morbidity and mortality following acute myocardial infarction. *J Am Coll Cardiol*. 2023;82:971–981. doi:10.1016/j.jacc.2023.06.024
- Krittawong C, Khawaja M, Tamis-Holland JE, et al. Acute myocardial infarction: etiologies and mimickers in young patients. *J Am Heart Assoc*. 2023;12:e029971. doi:10.1161/JAHA.123.029971
- Saito Y, Oyama K, Tsujita K, et al. Treatment strategies of acute myocardial infarction: updates on revascularization, pharmacological therapy, and beyond. *J Cardiol*. 2023;81:168–178. doi:10.1016/j.jcc.2022.07.003
- Li D, Tian K, Guo J, et al. Growth factors: avenues for the treatment of myocardial infarction and potential delivery strategies. *Regener Med*. 2022;17:561–579. doi:10.2217/rme-2022-0007
- Liu X, Wang L, Wang Y, et al. Myocardial infarction complexity: a multi-omics approach. *Clin Chim Acta*. 2024;552:117680. doi:10.1016/j.cca.2023.117680
- Czabotar PE, Garcia-Saez AJ. Mechanisms of BCL-2 family proteins in mitochondrial apoptosis. *Nat Rev Mol Cell Biol*. 2023;24:732–748. doi:10.1038/s41580-023-00629-4
- Niu N, Miao H, Ren H. Effect of miR-182-5p on apoptosis in myocardial infarction. *Heliyon*. 2023;9:e21524. doi:10.1016/j.heliyon.2023.e21524
- Liu Y, Shao YH, Zhang JM, et al. Macrophage CARD9 mediates cardiac injury following myocardial infarction through regulation of lipocalin 2 expression. *Signal Transduct Target Ther*. 2023;8:394. doi:10.1038/s41392-023-01635-w
- Duan J, Zhu D, Zheng X, et al. *Siraitia grosvenorii* (Swingle) C. Jeffrey: research progress of its active components, pharmacological effects, and extraction methods. *Foods*. 2023;13:12. doi:10.3390/foods13010012
- Gong X, Chen N, Ren K, et al. The fruits of *siraitia grosvenorii*: a review of a Chinese food-medicine. *Front Pharmacol*. 2019;10:1400. doi:10.3389/fphar.2019.01400
- Liang H, Cheng R, Wang J, et al. Mogrol, an aglycone of mogrosides, attenuates ulcerative colitis by promoting AMPK activation. *Phytomedicine*. 2021;81:153427. doi:10.1016/j.phymed.2020.153427
- Li H, Liu L, Chen HY, et al. Mogrol suppresses lung cancer cell growth by activating AMPK-dependent autophagic death and inducing p53-dependent cell cycle arrest and apoptosis. *Toxicol Appl Pharmacol*. 2022;444:116037. doi:10.1016/j.taap.2022.116037
- Chen Y, Zhang L, Li Z, et al. Mogrol attenuates osteoclast formation and bone resorption by inhibiting the TRAF6/MAPK/NF-κB signaling pathway in vitro and protects against osteoporosis in postmenopausal mice. *Front Pharmacol*. 2022;13:803880. doi:10.3389/fphar.2022.803880

14. Ju P, Ding W, Chen J, et al. The protective effects of Mogroside V and its metabolite 11-oxo-mogrol of intestinal microbiota against MK801-induced neuronal damages. *Psychopharmacology (Berl)*. 2020;237:1011–1026. doi:10.1007/s00213-019-05431-9
15. Cai X, He L, Zhou G, et al. Mogroside II ameliorates cardiomyopathy by suppressing cardiomyocyte apoptosis in a type 2 diabetic model. *Front Pharmacol*. 2021;12:650193. doi:10.3389/fphar.2021.650193
16. Miyatake S, Kato M, Kumamoto T, et al. De novo ATP1A3 variants cause polymicrogyria. *Sci Adv*. 2021;7. doi:10.1126/sciadv.abd2368
17. Boonsimma P, Michael Gasser M, Netbaram W, et al. Mutational and phenotypic expansion of ATP1A3-related disorders: report of nine cases. *Gene*. 2020;749:144709. doi:10.1016/j.gene.2020.144709
18. Moya-Mendez ME, Ogbonna C, Ezekian JE, et al. ATP1A3-encoded sodium-potassium ATPase subunit alpha 3 D801N variant is associated with shortened QT interval and predisposition to ventricular fibrillation preceded by bradycardia. *J Am Heart Assoc*. 2021;10:e019887. doi:10.1161/JAHA.120.019887
19. Mei B, Li J, Zuo Z. Dexmedetomidine attenuates sepsis-associated inflammation and encephalopathy via central α_2A adrenoceptor. *Brain Behav Immun*. 2021;91:296–314. doi:10.1016/j.bbi.2020.10.008
20. Khandibharad S, Singh S. Immuno-metabolic signaling in leishmaniasis: insights gained from mathematical modeling. *Bioinform Adv*. 2023;3:vbadi125. doi:10.1093/bioadv/vbadi125
21. Gustavsson EK, Zhang D, Reynolds RH, et al. ggtranscript: an R package for the visualization and interpretation of transcript isoforms using ggplot2. *Bioinformatics*. 2022;38:3844–3846. doi:10.1093/bioinformatics/btac409
22. Liu S, Wang Z, Zhu R, et al. Three differential expression analysis methods for RNA sequencing: limma, EdgeR, DESeq2. *J Vis Exp*. 2021:e62528.
23. Yu G, Wang LG, Han Y, et al. clusterProfiler: an R package for comparing biological themes among gene clusters. *Omic*. 2012;16:284–287. doi:10.1089/omi.2011.0118
24. Nolan T, Hands RE, Bustin SA. Quantification of mRNA using real-time RT-PCR. *Nat Protoc*. 2006;1:1559–1582. doi:10.1038/nprot.2006.236
25. Olsen MB, Kong XY, Louwe MC, et al. SLAMF1-derived peptide exhibits cardio protection after permanent left anterior descending artery ligation in mice. *Front Immunol*. 2024;15:1383505. doi:10.3389/fimmu.2024.1383505
26. Wang X, Wei Z, Wang P, et al. Echocardiographic evaluation of cardiac reserve to detect subtle cardiac dysfunction in mice. *Life Sci*. 2023;331:122079. doi:10.1016/j.lfs.2023.122079
27. Pan Y, Zhou Z, Zhang H, et al. The ATRQβ-001 vaccine improves cardiac function and prevents postinfarction cardiac remodeling in mice. *Hypertens Res*. 2019;42:329–340. doi:10.1038/s41440-018-0185-3
28. Zhang H, Dhalla NS, Li Y. The role of pro-inflammatory cytokines in the pathogenesis of cardiovascular disease. *Int J mol Sci*. 2024;26(1):25. doi:10.3390/ijms26010025
29. Jaiswal V, Lee HJ, Kushwaha PP. Pharmacological activities of mogrol: potential phytochemical against different diseases. *Life*. 2023;14(1):13. doi:10.3390/life14010013
30. Song JR, Li N, Wei YL, et al. Design and synthesis of mogrol derivatives modified on a ring with anti-inflammatory and anti-proliferative activities. *Bioorg Med Chem Lett*. 2022;74:128924. doi:10.1016/j.bmcl.2022.128924
31. Yin Y, Han W, Cao Y. Association between activities of SOD, MDA and Na(+)-K(+)-ATPase in peripheral blood of patients with acute myocardial infarction and the complication of varying degrees of arrhythmia. *Hellenic J Cardiol*. 2019;60(6):366–371. doi:10.1016/j.hjc.2018.04.003
32. Despa S, Bers DM. Na⁺ transport in the normal and failing heart - remember the balance. *J mol Cell Cardiol*. 2013;61:2–10. doi:10.1016/j.jmcc.2013.04.011
33. Shattock MJ, Ottolia M, Bers DM, et al. Na⁺/Ca²⁺ exchange and Na⁺/K⁺-ATPase in the heart. *J Physiol*. 2015;593:1361–1382. doi:10.1113/jphysiol.2014.282319
34. Wal P, Aziz N, Singh YK, et al. Myocardial infarction as a consequence of mitochondrial dysfunction. *Curr Cardiol Rev*. 2023;19:23–30. doi:10.2174/1573403X19666230508114311
35. Li Z, Xiao G, Wang H, et al. A preparation of Ginkgo biloba L. leaves extract inhibits the apoptosis of hippocampal neurons in post-stroke mice via regulating the expression of Bax/Bcl-2 and Caspase-3. *J Ethnopharmacol*. 2021;280:114481. doi:10.1016/j.jep.2021.114481
36. Li HR, Zheng XM, Liu Y, et al. L-carnitine alleviates the myocardial infarction and left ventricular remodeling through Bax/Bcl-2 signal pathway. *Cardiovasc Ther*. 2022;2022:9615674. doi:10.1155/2022/9615674
37. Wan X, Jin X, Wu X, et al. Ginsenoside Rd reduces cell proliferation of non-small cell lung cancer cells by p53-mitochondrial apoptotic pathway. *Heliyon*. 2024;10:e32483. doi:10.1016/j.heliyon.2024.e32483
38. Chen L, Li S, Zhu J, et al. Mangiferin prevents myocardial infarction-induced apoptosis and heart failure in mice by activating the Sirt1/FoxO3a pathway. *J Cell Mol Med*. 2021;25:2944–2955. doi:10.1111/jcmm.16329
39. Gang D, Qing O, Yang Y, et al. Cyanidin prevents cardiomyocyte apoptosis in mice after myocardial infarction. *Naunyn Schmiedeberg Arch Pharmacol*. 2024;397:5883–5898. doi:10.1007/s00210-024-02975-2
40. Li YW, Chen SX, Yang Y, et al. Colchicine inhibits NETs and alleviates cardiac remodeling after acute myocardial infarction. *Cardiovasc Drugs Ther*. 2024;38:31–41. doi:10.1007/s10557-022-07326-y

Drug Design, Development and Therapy

Publish your work in this journal

Drug Design, Development and Therapy is an international, peer-reviewed open-access journal that spans the spectrum of drug design and development through to clinical applications. Clinical outcomes, patient safety, and programs for the development and effective, safe, and sustained use of medicines are a feature of the journal, which has also been accepted for indexing on PubMed Central. The manuscript management system is completely online and includes a very quick and fair peer-review system, which is all easy to use. Visit <http://www.dovepress.com/testimonials.php> to read real quotes from published authors.

Submit your manuscript here: <https://www.dovepress.com/drug-design-development-and-therapy-journal>

Dovepress
Taylor & Francis Group